Journal of Alloys and Compounds 508 (2010) 20–23

Contents lists available at ScienceDirect

Journal of Alloys and Compounds

journal homepage: www.elsevier.com/locate/jallcom

Novel RZn_2Ga_2 (R = La, Ce, Pr, Nd, Sm) intermetallic compounds with $BaAl_4$-type structure

Yu. Verbovytskyy[a,*], D. Kaczorowski[b], A.P. Gonçalves[a]

[a] Departamento de Química, Instituto Tecnológico e Nuclear/CFMC-UL, Estrada Nacional 10, P-2686-953 Sacavém Codex, Portugal
[b] Institute of Low Temperature and Structure Research, Polish Academy of Sciences, P.O. Box 1410, 50-950 Wroclaw, Poland

ARTICLE INFO

Article history:
Received 13 July 2010
Received in revised form 29 July 2010
Accepted 30 July 2010
Available online 19 August 2010

Keywords:
Rare earth alloys and compounds
Crystal structure
X-ray diffraction
Magnetic measurements

ABSTRACT

Novel RZn_2Ga_2 intermetallics with R = La, Ce, Pr, Nd, Sm have been synthesized and characterized with regards to their crystal structures and magnetic properties. The compounds form with a tetragonal structure of the $BaAl_4$ type (space group *I4/mmm*). Except for $LaZn_2Ga_2$, they exhibit localised magnetism due to the presence of magnetic moments on the respective trivalent rare earth ions. The Pr-, Nd- and Sm-based compounds order antiferromagnetically at low temperatures with likely contribution of some ferromagnetic components.

1. Introduction

Albeit being the most effective way to identify new compounds with unusual crystallographic and physical properties, a systematic investigation among the components in the ternary R–Zn–Ga systems (R stands for a rare earth atom), including the construction of isothermal section and the determination of composition and crystal structure of ternary compounds, has not been intensively carried out. In the Yb–Zn–Ga system the isothermal section was built at 400 °C in the 0–33.3 at.% Yb composition range and four new ternary phases were indentified [1]: $YbZn_{0.25-0.5}Ga_{3.75-3.5}$ ($CaCu_{0.15}Ga_{3.85}$-type), $YbZn_{0.75-2}Ga_{3.25-2}$ ($BaAl_4$-type), $Yb_3Zn_{7.5-6.8}Ga_{3.5-4.2}$ (La_3Al_{11}-type) and $YbZn_{9.2-8.3}Ga_{1.8-2.7}$ ($BaHg_{11}$-type). The preudobinary RZn_2–RGa_2 (R = Ce, Sm, Gd, Er and Tm) systems were studied in order to determine the crystal structure and the extension of homogeneity ranges of the intermediate phases [2]: $CeCu_2$-type ($CeZn_{1.1-2}Ga_{0.9-0}$, $SmZn_{1.25-2}Ga_{0.75-0}$, $GdZn_{1.35-2}Ga_{0.65-0}$, $ErZn_{1.5-2}Ga_{0.5-0}$, $TmZn_{1.5-2}Ga_{0.5-0}$), AlB_2-type ($CeZn_{0-0.2}Ga_{2-1.8}$, $SmZn_{0-0.1}Ga_{2-1.9}$), $CaIn_2$-type ($CeZn_{0.6-1}Ga_{1.3-1}$, $SmZn_{0.7-1.2}Ga_{1.3-0.8}$, $GdZn_{0.7-1.2}Ga_{1.3-0.8}$, $ErZn_{0.7-1.4}Ga_{1.3-0.6}$, $TmZn_{0.6-1.4}Ga_{1.4-0.6}$), $CeCd_2$-type ($SmZn_{0.3-0.6}Ga_{1.7-1.4}$, $GdZn_{0.3-0.6}Ga_{1.7-1.4}$, $ErZn_{0.2-0.6}Ga_{1.8-1.4}$, $TmZn_{0.1-0.6}Ga_{1.9-1.4}$). The crystal structure of the $CeCu_2$ type and the physical properties of equiatomic gallide EuZnGa were communicated in Ref. [3]. Moreover, the formation of a new ternary phase crystallizing with the MoB structure type was reported in Ref. [4] as a result of the investigation of cross-section YZn–YGa. Complete crystal structure determination has been done for the composition $YZn_{0.2}Ga_{0.8}$.

The present work aimed at investigations of the crystal structures and the magnetic properties of the new RZn_2Ga_2 (R = La, Ce, Pr, Nd, Sm) compounds.

2. Experimental details

Metals with nominal purities >99.95 wt.% (rare earth ingots, zinc tear drops and gallium pieces) were used as starting materials. Each RZn_2Ga_2 (R = La, Ce, Pr, Nd, Sm) sample was synthesized by melting the elements inside quartz ampoules under vacuum (10^{-5} Torr). The reactions were first performed at 900–950 °C, the ampoules being held at that temperature for 1 h, followed by their cooling to 400–500 °C in air, and subsequent quenching in cold water. The so-obtained samples had metallic-like lustres. No reaction with walls of the quartz ampoules was observed. In the next step, fragments of the prepared ingots were sealed in evacuated quartz tubes and annealed at 400 °C for 20 days, inside a vertical oven. The samples were quenched by submerging the quartz tubes in cold water.

Quality of the final products was examined by X-ray powder diffraction using a PANalytical X'Pert Pro diffractometer (Cu Kα-radiation). The scans were taken in the $\theta/2\theta$ mode within the 2θ region of 15–120° (step scan, 0.03°; counting time per step, 20 s). The theoretical powder patterns were calculated with the help of the PowderCell program [5] and used for the identification of the phases. The lattice parameters were obtained by least-squares fitting using the Latcon program [6]. The FullProf program [7] was used for the Rietveld fittings. Pseudo-Voigt profile shape function was assumed. The background was refined with a polynomial function. Details of data refinements are given in Table 1.

Magnetic measurements were performed in the temperature range 1.7–400 K and in magnetic fields up to 5 T using a Quantum Design MPMP-5 SQUID magnetometer.

* Corresponding author.
E-mail address: yuryvv@bigmir.net (Yu. Verbovytskyy).

0925-8388/$ – see front matter © 2010 Elsevier B.V. All rights reserved.
doi:10.1016/j.jallcom.2010.07.227

Table 1
Structural data of RZn_2Ga_2 phases ($BaAl_4$ structure type, $I4/mmm$ space group, $Z = 2$).

Phase	$LaZn_2Ga_2$	$CeZn_2Ga_2$	$PrZn_2Ga_2$	$NdZn_2Ga_2$	$SmZn_2Ga_2$
Lattice parameters					
a (Å)	4.3015(1)	4.2600(1)	4.2410(1)	4.2103(1)	4.1714(1)
c (Å)	10.7253(3)	10.7192(3)	10.7317(3)	10.7663(4)	10.7977(2)
V (Å^3)	198.45(1)	194.53(1)	193.02(1)	190.85(1)	187.88(1)
ρ_{cal} (g/cm^3)	6.846	7.005	7.073	7.211	7.433
Reliability factors					
R_B, R_F (%)	4.65, 3.27	4.68, 2.95	5.07, 3.02	4.84, 3.37	5.75, 4.29
R_p, R_{wp} (%)	9.14, 12.6	9.68, 12.3	7.74, 10.3	9.01, 13.2	9.22, 12.0
χ^2	9.72	5.23	4.69	10.7	5.21
Atom positions					
R (0, 0, 0), B_{iso} (Å^2)	0.85(4)	0.91(3)	0.95(3)	1.01(5)	0.85(4)
M1 (0, 1/2, 1/4), B_{iso} (Å^2)	1.35(5)	1.54(5)	1.31(4)	1.33(6)	1.44(4)
M2 (0, 0, z), B_{iso} (Å^2)	0.3826(2), 0.94(6)	0.3834(1), 0.89(4)	0.3851(1), 0.89(4)	0.3853(2), 0.70(7)	0.3866(1), 0.75(5)

M = 0.5Zn + 0.5 Ga.

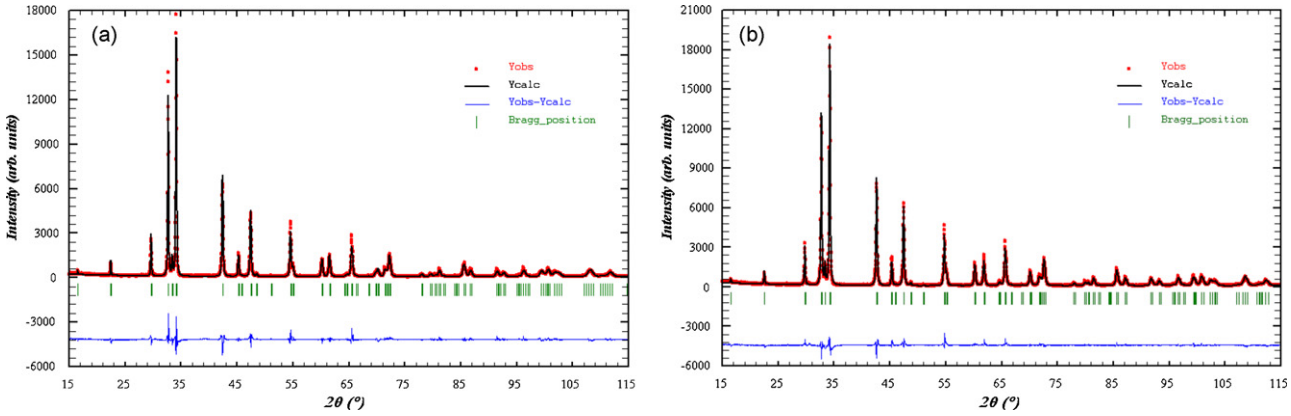

Fig. 1. Rietveld profile refinements of the X-ray diffraction data for $CeZn_2Ga_2$ (a) and $PrZn_2Ga_2$ (b).

3. Results and discussion

3.1. Crystal structure

The X-ray powder diffraction data of all the RZn_2Ga_2 (R = La, Ce, Pr, Nd, Sm) alloys can be indexed within a tetragonal unit cell, with the c/a ratios and the Bragg peaks intensities characteristic of the $BaAl_4$ structure type. The crystal structure refinements performed by the Rietveld method confirmed this structure type and yielded the structural parameters listed in Table 1. As an example, the results of the Rietveld profile refinements of the X-ray diffraction data collected for $CeZn_2Ga_2$ and $PrZn_2Ga_2$ are displayed in Fig. 1.

In the $BaAl_4$-type unit cell of RZn_2Ga_2, the rare earth atoms occupy the positions of Ba atoms (2a), while the Zn and Ga atoms are statistically distributed over the positions of Al atoms (4d and 4e). Because of small difference in the scattering factors between zinc and gallium, refinement of the occupation coefficients for the 4d and 4e sites cannot give any statistically relevant indication of a preferred occupation of one of these positions. The statistical mixtures of the Zn and Ga atoms were thus fixed during the calculations and presented as M = 0.5Zn + 0.5Ga.

The unit cell and the coordination polyhedra of the atoms are presented in Fig. 2. The neighbours of the R atoms form 22-vertex polyhedra. The M1 atoms are located inside cubooctahedra (coordination number 12). The coordination spheres of the M2 atoms have a form of tri-capped trigonal prisms (coordination number 9).

Fig. 3 shows the variation of the unit cell volume as a function of the atomic number. Apparently, the volume gradually decreases along the R series, just in agreement with the so-called lanthanide contraction mechanism.

The interatomic distances are gathered for all the compounds in Table 2. The shortest R–M distances range from 3.292 Å in $LaZn_2Ga_2$ to 3.194 Å in $SmZn_2Ga_2$. For the latter alloy the Sm–M bonds are shorter than the sums of the atomic radii $r_{sm} + r_{Zn,Ga} = 3.20$ Å [8]. For $NdZn_2Ga_2$ the Nd–M distance is closed to the sum $r_{Nd} + r_{Zn,Ga} = 3.21$ Å [8]. For the other compounds the separation of the R and M atoms is larger than the respective sums of the atomic radii.

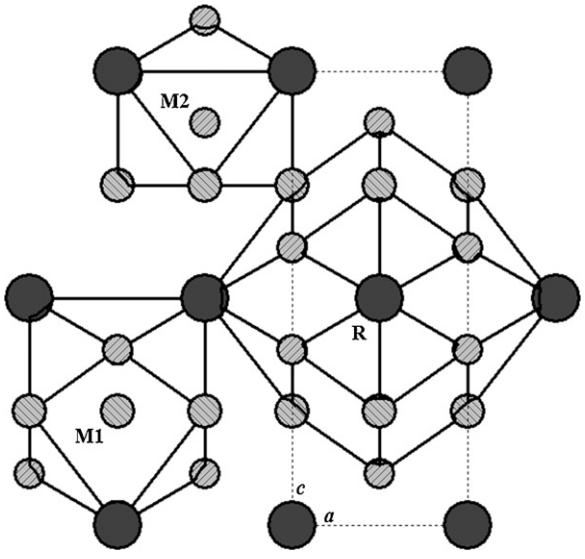

Fig. 2. Unit cell of the ternary compounds RZn_2Ga_2 and the coordination polyhedra of the atoms: R (dark circles) and M (Zn and Ga) (light circles).

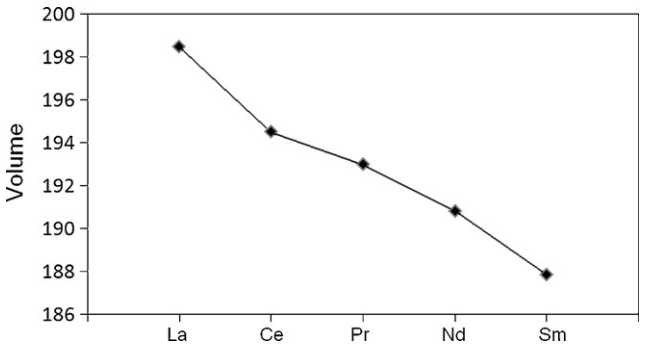

Fig. 3. Unit cell volume (Å^3) vs. atomic number for the series of RZn_2Ga_2 compounds.

Table 2
Interatomic distances in RZn_2Ga_2 compounds.

Bonds	$LaZn_2Ga_2$	$CeZn_2Ga_2$	$PrZn_2Ga_2$	$NdZn_2Ga_2$	$SmZn_2Ga_2$	CN
R–						
–8 M2	3.292(1)	3.261(1)	3.242(1)	3.223(1)	3.194(1)	22
–8 M1	3.437(1)	3.423(1)	3.420(1)	3.417(1)	3.411(1)	
–2 M2	4.103(2)	4.110(1)	4.133(1)	4.148(2)	4.174(1)	
–4 R	4.301(1)	4.260(1)	4.241(1)	4.210(1)	4.171(1)	
M1–						
–4 M2	2.578(1)	2.565(1)	2.569(1)	2.560(1)	2.555(1)	12
–4 M1	3.042(1)	3.012(1)	2.999(1)	2.977(1)	2.950(1)	
–4 R	3.437(1)	3.423(1)	3.420(1)	3.417(1)	3.411(1)	
M2–						
–M2	2.518(3)	2.500(2)	2.466(2)	2.470(3)	2.449(2)	9
–4 M1	2.578(1)	2.565(1)	2.569(1)	2.560(1)	2.555(1)	
–4 R	3.292(1)	3.261(1)	3.242(1)	3.223(1)	3.194(1)	

The Zn and Ga atoms form three-dimensional networks. The M1–M1 distances are about 3.00 Å, i.e. they are larger than those observed in pure metals ($2r_{Zn} \approx 2r_{Ga} \approx 2.78$ Å) [8]. The shortest M1–M2 and M2–M2 bonds are shorter than 2.78 Å. Along the RZn_2Ga_2 series these distances change from 2.555 Å to 2.578 Å and from 2.449 Å to 2.518 Å, respectively, i.e. they are reduced with respect to those in pure metals by about 8% and 11%, respectively. Such bond contractions are typical for intermetallics crystallizing with the $BaAl_4$-type crystal structure [9].

According to the data bases (see e.g. Ref. [9]), there exists a large family of intermetallic rare earth – (d-metal) – (p-metal) phases which form with the $BaAl_4$-type or related structures. The occupation preferences of the d- and p-metals in these phases are complex and depend on the atomic size and the relative electronegativities of the elements. However, some of them, with composition RTX_3 and RT_2X_2 (R – rare earth, T – d- and X – p-metals), prefer forming ordered structures, such as $ThCr_2Si_2$-, $CaBe_2Ge_2$-, $BaNiSn_3$- and $CePtGa_3$-types [10]. Häussermann et al. [11] suggested that elements with larger electronegativity prefer to occupy 4e position. For example, one finds $(La)^{2a}(Al)^{4d}(Zn)^{4e}$, $(Ce)^{2a}(Al)^{4d}(Zn)^{4e}$, $(Pr)^{2a}(Al)^{4d}(Zn)^{4e}$, $(Sm)^{2a}(Al)^{4d}(Zn)^{4e}$,

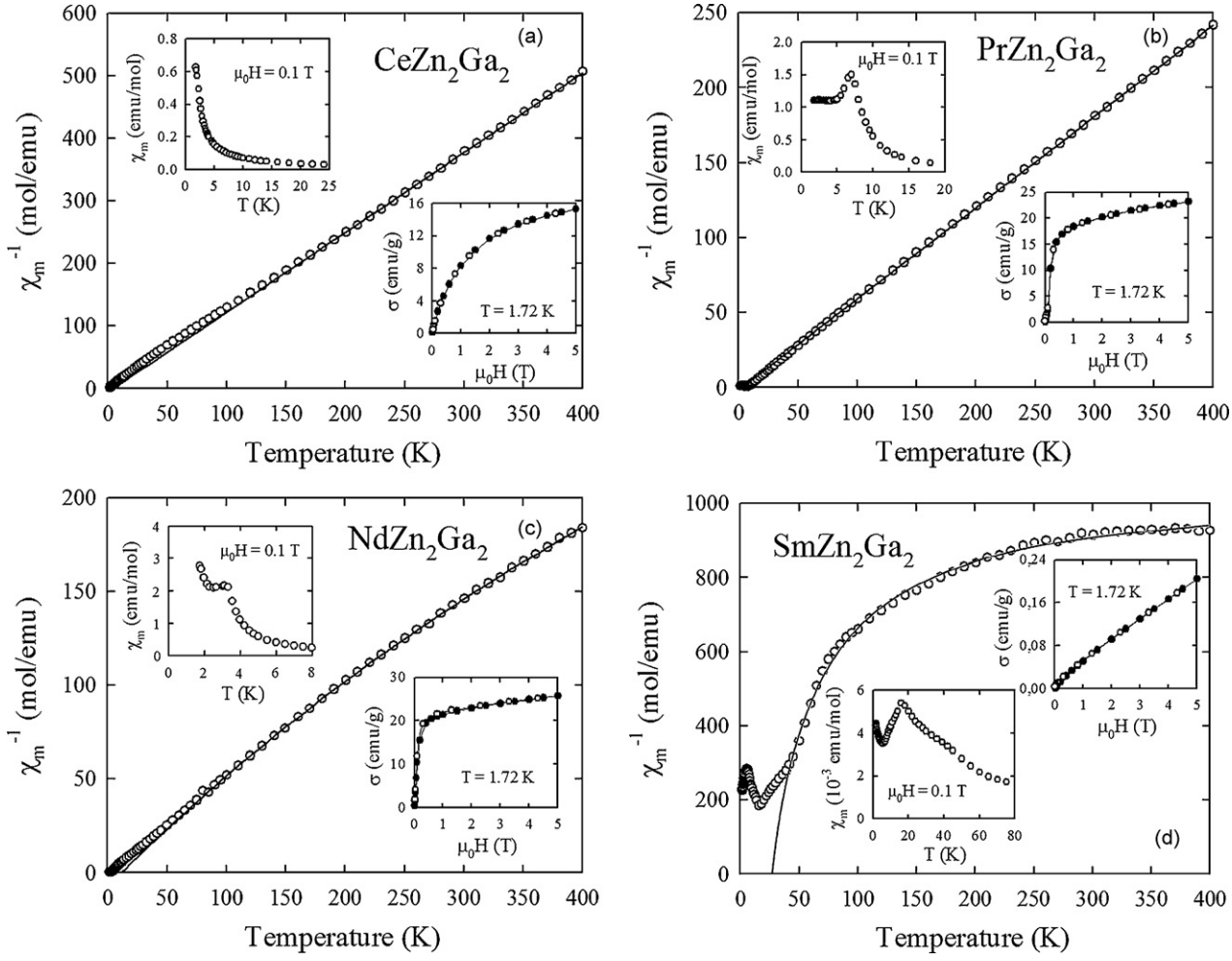

Fig. 4. Temperature dependencies of the inverse molar magnetic susceptibility of (a) $CeZn_2Ga_2$, (b) $PrZn_2Ga_2$, (c) $NdZn_2Ga_2$ and (d) $SmZn_2Ga_2$. The solid curves are the Curie–Weiss fits discussed in the text. The insets display the magnetic susceptibility at low temperatures and the magnetization isotherms measured at 1.72 K with increasing (full symbols) and decreasing (open symbols) magnetic field.

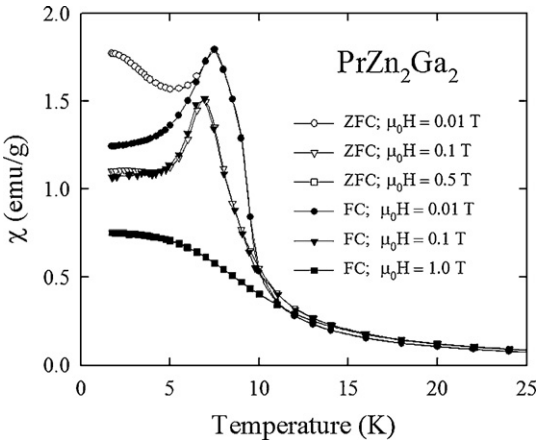

Fig. 5. Low-temperature variations of the mass magnetic susceptibility of $PrZn_2Ga_2$ measured in various magnetic fields upon cooling the sample in zero (ZFC) and applied field (FC).

$(Nd)^{2a}(Al)^{4d}(0.83Zn + 0.17Al)^{4e}$, $(Sm)^{2a}(Al)^{4d}(0.9Zn + 0.1Al)^{4e}$ and $(Yb)^{2a}(0.05Zn + 0.95Al)^{4d}(0.77Zn + 0.23Al)^{4e}$ for $LaZn_2Al_2$, $CeZn_2Al_2$, $PrZn_2Al_2$, $SmZn_2Al_2$, $NdZn_{1.66}Al_{2.34}$, $SmZn_{1.68}Al_{2.32}$ and $YbZn_{1.65}Al_{2.35}$ [12,13 and references therein] respectively. However, in the case of RZn_2Ga_2 compounds it is difficult to predict the d- and p-metals site preferences based on this approach, as Zn and Ga have similar electronegativities.

3.2. Magnetic properties

The magnetic measurements of $LaZn_2Ga_2$ revealed that it is a weak diamagnet with the molar susceptibility of about -3.5×10^{-4} emu/mol (not shown). In turn, the magnetic susceptibility of $CeZn_2Ga_2$ (shown in Fig. 4a) follows above about 100 K the Curie–Weiss law, with the effective magnetic moment $\mu_{eff} = 2.50\,\mu_B$ and the paramagnetic Curie temperature $\theta = 4.4$ K. The experimental value of μ_{eff} is close to that expected for a Ce^{3+} ion, while the positive value of θ may indicate some ferromagnetic correlations. However, as displayed in the upper inset of Fig. 4a, the compound remains paramagnetic down to 1.72 K. Also the field variation of the magnetization, taken at the lowest temperature (see the lower inset of Fig. 4a), is consistent with the paramagnetic ground state. The observed deviation of the $\chi^{-1}(T)$ curve from the straight-line behaviour is likely caused by crystal field interactions.

The temperature dependence of the inverse molar magnetic susceptibility of $PrZn_2Ga_2$ is presented in Fig. 4b. Above about 50 K, it can be described by the Curie–Weiss law, with the parameters $\mu_{eff} = 3.62\,\mu_B$ and $\theta = 2.8$ K. The value of μ_{eff} indicates trivalent Pr ions. As apparent from the inset of Fig. 4b, the compound orders antiferromagnetically at $T_N = 7$ K. The antiferromagnetic order is corroborated by a metamagnetic transition observed in the field-dependent magnetization isotherm measured at 1.72 K. At this temperature, the critical field is about 0.1 T, and the magnetic moment measured in a field of 5 T is about $1.7\,\mu_B$. The latter value is much smaller than that expected for the $^3H_4$ multiplet of free Pr^{3+} ions, and should be referred to the crystal field ground state. The positive value of the paramagnetic Curie temperature hints at some ferromagnetic interactions. Indeed, some bifurcation of the magnetic susceptibility curves taken in the zero-field-cooling (ZFC) and field-cooling (FC) regimes in weak magnetic fields (Fig. 5) manifests the presence of a small ferromagnetic component in the nominally antiferromagnetic structure of $PrZn_2Ga_2$.

Fairly complex magnetic behaviour was also revealed for $NdZn_2Ga_2$. As can be inferred from Fig. 4c (see the upper inset), the compound orders antiferromagnetically at $T_N = 3$ K, yet below 2 K the magnetic susceptibility exhibits an upturn that hints at some change in the magnetic structure possibly caused by interplay of antiferromagnetic and ferromagnetic components, as suggested for the Pr-based counterpart. Also for this compound, the magnetic state is very sensitive to applied magnetic field: above 1 kOe a field-induced ferromagnetism is observed at $T = 1.72$ K with a large magnetic moment of about $2\,\mu_B$ in the field $\mu_0 H = 5$ T (see the lower inset of Fig. 4c). In the paramagnetic region, the magnetic susceptibility of $NdZn_2Ga_2$ can be described by a modified Curie–Weiss law with the parameters $\mu_{eff} = 3.58\,\mu_B$, $\theta = 11.5$ K and $\chi_0 = 1.31 \times 10^{-3}$ emu/mol. The experimental effective magnetic moment is close to the theoretical Nd^{3+} ion value, while the paramagnetic Curie temperature is positive and relatively large, in agreement with the behaviour of the compound in the ordered state.

The magnetic properties of $SmZn_2Ga_2$ are summarized in Fig. 4d. The compound exhibits antiferromagnetism below $T_N = 16$ K with an upturn in the magnetic susceptibility below 5 K that may be due to spin reorientation. At 1.72 K, the magnetization is nearly proportional to the magnetic field strength that is in line with the antiferromagnetic ground state. A hump in the susceptibility near 40 K has unclear origin. In the paramagnetic range, the magnetic susceptibility varies in a manner characteristic of Sm-based compounds. The observed strong curvature of $\chi^{-1}(T)$ is a direct consequence of the closeness in energy of the $^6H_{5/2}$ and $^6H_{7/2}$ terms of the Sm^{3+} ground multiplet. Applying the modified Curie–Weiss formula to the data above 50 K yielded $\mu_{eff} = 0.56\,\mu_B$, $\theta = 27.2$ K and $\chi_0 = 9.56 \times 10^{-4}$ emu/mol. The value of μ_{eff} is somewhat smaller than that expected for a trivalent Sm ion ($0.84\,\mu_B$), possibly because of the impurity contribution that may be associated with the anomaly near 40 K.

Acknowledgments

This work was partially supported by FCT, Portugal, under the contract No. PTDC/QUI/65369/2006. The FCT Grant No. SFRH/BPD/34840/2007 for the research work of Y.V. at ITN, Sacavém, Portugal is highly appreciated. Part of the work was done in the frame of the Executive Programme of Scientific and Technological Cooperation between Portugal and Poland for the years 2009–2010.

References

[1] Yu. Verbovytskyy, A.P. Gonçalves, Intermetallics 18 (2010) 655–665.
[2] A. Iandelli, J. Less-Common Met. 169 (1991) 187–196.
[3] R. Pöttgen, G. Kotzyba, F.M. Schappacher, B.D. Mosel, H. Eckert, Yu. Grin, Z. Anorg. Allg. Chem. 627 (2001) 1299–1304.
[4] J.-T. Zhao, D.-K. Seo, J.D. Corbett, J. Alloys Compd. 334 (2002) 110–117.
[5] G. Nolze, W. Kraus, Powder Cell for Windows, Federal Institute for Materials Research and Testing, Berlin, 1999 (Version 2.3).
[6] D. Schwarzenbach, Program LATCON, University of Lausanne, Switzerland, 1975.
[7] J. Rodriguez-Carvajal, T. Roisnel, FullProf.98 and WinPLOTR: New Windows 95/NT Applications for Diffraction Commission For Powder Diffraction, International Union for Crystallography, Newsletter No. 20 (May–August) Summer, 1998.
[8] G.B. Bokiy, Kristallohimiya (Crystal Chemistry), 3rd ed., Nauka, Moscow, 1971, in Russian.
[9] P. Villars (Ed.), Pearson's Handbook, Crystallographic Data for Intermetallic Phases, desk ed., ASM Materials Park, OH, 1997.
[10] E. Parthé, L. Gelato, B. Chabot, M. Penzo, K. Cenzual, R. Gladyshevskii, TYPIX, Standardized Data and Crystal Chemical Characterization of Inorganic Structure Types, Springer-Verlag, Berlin, 1994.
[11] U. Häussermann, S. Amerioun, L. Eriksson, C.-S. Lee, G.J. Miller, J. Am. Chem. Soc. 124 (2002) 4371–4383.
[12] G. Cordier, E. Czech, H. Schäfer, P. Woll, J. Less-Common Met. 110 (1985) 327–330.
[13] B. Stel'makhovych, O. Stel'makhovych, Yu. Kuz'ma, J. Alloys Compd. 397 (2005) 115–119.